N84-27858

NASA Technical Memorandum 83672

Modeling Degradation and Failure of Ni-Cr-Al Overlay Coatings

J. A. Nesbitt
Lewis Research Center
Cleveland, Ohio

and

R. W. Heckel
Michigan Technological University
Houghton, Michigan

Prepared for the
Eleventh International Conference on Metallurgical Coatings
sponsored by the American Vacuum Society
San Diego, California, April 9-13, 1984

NASA

MODELING DEGRADATION AND FAILURE OF Ni-Cr-Al OVERLAY COATINGS

J. A. Nesbitt
National Aeronautics and Space Administration
Lewis Research Center
Cleveland, Ohio 44135

and

R. W. Heckel
Michigan Technological University
Houghton, Michigan 49931

E-2116

SUMMARY

Degradation of a Ni-16Cr-25Al-0.06Zr overlay coating on a Ni-22Cr substrate was examined after oxidation accompanied by thermal cycling. Concentration/distance profiles were measured in the coating and substrate after various 1-hr cycles at 1150° C. A numerical model was developed to simulate coating degradation by simultaneous oxidation and coating/substrate interdiffusion. The validity of the model was confirmed by comparison of predicted and measured concentration/distance profiles. The ability of the model to identify critical system parameters was demonstrated for the case of the initial Al and Cr content of the coating and substrate.

INTRODUCTION

Nickel and cobalt-based overlay coatings are gaining increased use for oxidation and hot corrosion protection of high-temperature gas turbine components. The coatings are primarily used as an external metallic coating (refs. 1 to 4), but are seeing increased use and development as a bond coat between the superalloy substrate and an external ceramic layer for thermal barrier coatings (ref. 5). Overlay coatings typically contain 10 to 15 at. % Cr and 20 to 30 at. % Al and provide high-temperature protection by the selective oxidation of Al to form a continuous external scale of Al_2O_3 (ref. 1). The coatings usually contain a small amount (<1.0 at. %) of a reactive element (e.g, Y or Zr) which increases the adherence of the oxide scale to the metallic coating (refs. 6 and 7).

Both oxidation and coating/substrate interdiffusion degrade the coating by reducing the Al content of the coating (ref. 1). Thermal cycling accelerates the loss of Al from the coating due to repeated Al_2O_3 spallation and reformation. The more severe the oxide spallation, the more rapid the loss of Al from the coating. Coating/substrate interdiffusion can also result in the effective loss of Al from the coating and a reduction in the Al_2O_3-forming capability of the coating. The extent of coating/substrate interdiffusion is dependent on the oxidation temperature, the time at that temperature, and both the coating and substrate composition (ref. 8).

Continuous coating degradation results in failure of the coating to reform the protective Al_2O_3 scale. The failure to reform the Al_2O_3 scale is accompanied by formation of less protective oxides such as NiO, Cr_2O_3 and Ni spinels (ref. 9). The formation of less protective oxides can also result in internal oxidation of Al in the coating (refs. 9 and 10). The failure to reform the Al_2O_3 scale, and the formation of less protective surface oxides is commonly referred to as breakaway oxidation and is associated with rapid metal consumption of the coating, and eventually, the superalloy component.

Coating failure occurs due to insufficient Al transport in the coating towards the oxide scale (refs. 9 and 11). The inability of the coating to reform the Al_2O_3 scale is transport related and not solely dependent on the amount of Al remaining in the coating. The Al transport, and specifically the Al flux towards the Al interface is dependent on both the oxidation temperature (as it directly affects the diffusion coefficients) and the existing concentration/distance profiles in the coating (ref. 12).

The purpose of this paper is threefold: First, to briefly present the experimental results for a Ni-16Cr-25Al-0.06Zr* overlay coating on a Ni-22Cr substrate after oxidation accompanied by thermal cycling. Secondly, to discuss the development and predictions of a diffusion model capable of simulating overlay coating degradation by simultaneous oxidation and coating/substrate interdiffusion. The ability of the diffusion model to predict accurately diffusional transport is demonstrated by a comparison of predicted and measured Al and Cr concentration profiles. Thirdly, the ability of the model to identify critical system parameters is demonstrated by examining two system parameters, the initial Al and Cr content of the coating and substrate, and their effect on the protective life of the coating. The results presented in this paper are part of a larger study examining Ni-16Cr-25Al-0.06Zr overlay coating degradation on several Ni-Cr-Al substrates. The conclusions discussed later in this paper also apply to the various substrate compositions examined in the larger study (ref. 12).

EXPERIMENTAL PROCEDURE AND RESULTS

Cast bars of the Ni-22Cr substrate alloy were machined to a cylindrical geometry of approximately 0.64 cm diameter by 2.5 cm in length. The ends of the cylinders had been rounded before the coating was applied to reduce sharp corner effects on the oxide spalling behavior of the coated cylinders. The coating was applied by low-pressure plasma spraying. Composition of the coating after spraying was approximately Ni-16Cr-25Al-0.06Zr (ref. 12).

The as-sprayed coating was annealed in Ar at 1150° C for 2 hr to permit interdiffusion to improve the coating/substrate bond. After the anneal at 1150° C, the coating possessed a two-phase microstructure consisting of γ (FCC, Ni solid solution) and approximately 70 vol. % β (NiAl-type structure). The two-phase structure of the coating is evident in figure 1(a). Very little porosity was observed in the coating but porosity at the coating/substrate interface was evident after a short isothermal anneal (fig. 1(a)). The coating thickness was uniform about the circumference of each cylinder but

---

*All compositions are in atomic percent.

varied between specimens in the range 88 to 103 μm. Following the isothermal anneal, the specimens underwent cyclic oxidation consisting of 1-hr cycles at 1150° C in static air followed by a 20-min cooling period out of the furnace. The cylinders were periodically removed from the furnace and weighed in order to determine the weight change. The specimens underwent a total of 100, 200, or 250 thermal cycles. Further details of the cyclic oxidation testing are given elsewhere (refs. 12 and 13). After oxidation, the surface oxides were identified by X-ray diffraction (table I). Following the X-ray analysis of the surface oxides, the specimens were first Cu and then Ni plated to help retain the surface oxide scale during sectioning and polishing. The plated specimens were sectioned, mounted and polished by standard metallographic techniques and examined by optical metallography and electron microprobe analysis (ref. 12).

Oxidation and coating/substrate interdiffusion resulted in complete depletion of the high-Al β phase from the coating before 100 cycles. Previous work (ref. 12) has indicated that total β depletion would occur in less than 15 hr at 1150° C for the coating thickness examined in this study. No α-Cr (bcc) or γ' (Ni_3Al type structure) phases were observed in the coating after 100 cycles but may have formed and dissolved at shorter times (ref. 12). After 100 and 200 cycles significant porosity was evident at the coating/substrate interface as well as in the substrate. The porosity at the coating/substrate interface appeared to be almost continuous after 200 cycles. After 250 cycles, considerable oxide formation had occurred at the coating/substrate interface and internally in the coating and substrate (fig. 1(b)). The porosity at the coating/substrate interface resulted in delamination and spallation of the coating from the end of the cylinder (fig. 1(c)). Oxygen gaining entrance along the coating/substrate interface has diffused into the substrate internally oxidizing the Al which has diffused from the coating into the substrate and has also caused significant oxidation at the coating/substrate interface (fig. 1(b)).

The Al and Cr concentration profiles were measured in the coating and substrate after 100, 200 and 250 cycles using an electron microprobe and a ZAF correction routine (ref. 12). Two microprobe traces were made at different locations on each specimen and are shown in the following figures. The Al content of the coating decreased rapidly primarily as a result of coating/substrate interdiffusion. After 100 cycles the Al content of the coating decreased from 25 at. % to below 6 at. % (fig. 2(a)). After 200 cycles, the Al content had decreased to 2 to 4 at. % (fig. 2(b)), whereas after 250 cycles the Al was almost completely depleted from the coating (fig. 2(c)). The Cr concentration in the coating generally increased with increasing oxidation cycles via diffusion of Cr from the substrate into the coating (fig. 2(a) to (c)).

The slope of the Al concentration profile near the oxide/coating interface is indicative of the rate of Al consumption in the formation and growth of the Al_2O_3 scale (ref. 11). The relatively flat Al profile in the coating after 100 cycles indicates a low rate of Al transport to the oxide/coating interface associated with the low growth rate (and therefore low rate of Al consumption) of the Al_2O_3. The steeper Al concentration gradient at the oxide/coating interface after 200 cycles indicates a higher rate of Al consumption and reflects the formation of less protective oxide scales (see table I). In the cylinder oxidized for 250 cycles, Al loss due to oxidation at the oxide/coating interface, oxidation associated with the oxygen penetration along the coating/substrate interface, and coating/substrate interdiffusion have each contributed to reducing the Al transport to the oxide scale which has resulted in failure of the coating. As observed (table I, 250 cycles), less protective oxides formed when the coating was unable to supply sufficient Al to the oxide scale.

Numerical Modeling Results and Discussion

A numerical model (COSIM - Coating Oxidation and Substrate Interdiffusion Model) was developed to simulate overlay coating degradation by simultaneous oxidation and coating/substrate interdiffusion (ref. 12). A numerical model was necessary to deal with the inherent complexities of the problem which include a finite coating thickness, the concentration dependence of the four ternary interdiffusion coefficients for Al and Cr, and the boundary condition at the oxide/coating interface. Finite-difference techniques (refs. 14 and 15) were utilized in the model to provide a numerical solution to the ternary equivalent of Fick's second law. The COSIM model simulates the diffusional transport of both Al and Cr in the γ phase of the coating and substrate. The boundary condition at the oxide/coating interface was supplied by the Cyclic Oxidation Spalling Program (COSP) (ref. 16) as the rate of Al consumed during the growth and partial spallation of the Al_2O_3 scale.

Several assumptions were required in the development of the numerical model (ref. 12). Three of the more critical assumptions were

1. Only Al_2O_3 was formed.

2. The two-phase coating could be approximated as a single phase of equivalent Al and Cr content.

3. The ternary diffusivities for the γ phase could be extrapolated to the high Al concentration in the assumed single-phase coating layer.

These assumptions will be discussed shortly.

Parameters input to the COSIM model consist of the initial Al and Cr concentration of the coating and substrate, as well as the coating thickness. The model also requires the concentration dependence of the four ternary diffusion coefficients for the γ phase appropriate for the oxidation temperature. Input to the COSP spalling model consisted of a parabolic oxide growth constant, k_p and a spalling parameter, Q_o. The spalling parameter Q_o was chosen by matching the cylinder weight change predicted by COSP to the weight change data measured during cyclic oxidation.

The COSIM model predicts the Al and Cr concentration/distance profiles in the coating and in the substrate after a set number of oxidation cycles. More importantly, the model predicts the time variation of the Al concentration at the oxide/coating interface. When the Al concentration at the oxide/coating interface is approximately zero, further loss of Al from the coating by oxidation or interdiffusion causes the Al concentration gradient at the interface to decrease, reducing the Al flux (or rate of Al transport) to the oxide scale. The model predicts coating failure due to this lack of Al transport in the coating to the oxide scale, the time of coating failure being predicted when the Al concentration at the oxide/coating interface is approximately zero. (Thermodynamically, approximately 1 ppm of Al is the lower limiting Al concentration for Al_2O_3 to be the stable oxide phase formed on Ni-Cr-Al alloys at 1100° C (ref. 10). Technically, when the Al concentration at the oxide/coating interface decreased to 1 ppm of Al, coating failure would be predicted.)

Concentration/Distance Profiles

The concentration/distance profiles predicted by the COSIM model show excellent agreement with the measured profiles after 100 cycles (fig. 2(a)). The predicted profiles show reasonably good agreement after 200 cycles (fig. 2(b)) but poor agreement after 250 cycles (fig. 2(c)).

The observed agreement is not surprising considering the first assumption of the model that only Al_2O_3 was formed. After 100 cycles, Al_2O_3 was the major oxide phase detected on the specimen surface with some $NiAl_2O_4$ also present. After 200 cycles, Al_2O_3 was still the dominant oxide phase detected but with limited amounts of four other oxides also present. After 250 cycles, Cr_2O_3 was the dominant oxide phase detected on the specimen surface. In addition, the coating and substrate after 250 cycles were almost completely detached due to the porosity resulting from coating/substrate interdiffusion. The oxidation which occurred between the coating and substrate, and internally in the coating and substrate, reduced the Al content in both the coating and substrate below the model prediction.

The assumption that only Al_2O_3 had formed is obviously only an approximation, but as shown, the model predictions show very good agreement to the measured concentration profiles when Al_2O_3 was the major oxide phase present in the scale. Approximating the two-phase coating as a single phase, and extrapolating the ternary diffusivities to the Al and Cr concentrations in this phase appears justified considering the relatively short time the β phase exists in the coating undergoing cyclic oxidation at 1150° C. In summary, the numerical model has been shown to predict concentration profiles with reasonable success over the range of applicability of the model (where Al_2O_3 is the major phase present in the oxide scale).

Critical Parameters

The ability of the numerical model to identify critical parameters in coating/substrate systems which influence coating life (as limited by Al transport to the oxide scale) can be demonstrated for two system parameters, the initial Al and Cr concentrations in the coating and substrate. Other system parameters which could be examined by the COSIM model are the coating thickness, oxidation temperature, thermal cycle frequency, rate of oxide spallation, etc. The effect of the Al concentration on coating life can be shown by examining the time dependence of the Al concentration at the oxide/coating interface. The length of time for the Al concentration at this interface to decrease to zero is a measure of the protective life of the coating. The more rapid the concentration decrease, the shorter the coating life.

The model predicts that small increases in the Al content of the substrate have a greater effect on coating life than similar increases in the Al content of the coating. The effect of increasing the initial Al content of the coating is shown by the three centermost curves (20, 25, and 30 at. %) in figure 3(a) (substrate contains 4 at. % Al). As expected, the coating life is greatest for the coating with the highest Al content. Similarly, the effect of increasing the Al content of the substrate from 0 to 8 at. % (coating contains 25 at. % Al) is also shown in figure 3(a). It is obvious that an 8 at. % increase in the Al content of the substrate has a much greater effect on coating life than a 10 at. % increase in the Al content of the coating.

The model predicts the Cr content of the coating and substrate to have very little effect on the coating life. Variations in the Cr content of 0-20 at. % in the substrate and 10-20 at. % in the coating (spanning the concentration range for typical superalloy substrates and coatings) are shown in figure 3(b). The effect of varying the Cr concentration is relatively small when compared to the effect of varying the Al concentrations (fig. 3(a)). The limited effect of the Cr concentration is expected since the diffusivity of Al (D_{AlAl}) is only weakly dependent on the Cr concentration and since the Cr concentration gradient has only a small effect on the diffusion of Al (i.e., $D_{AlAl} \gg D_{AlCr}$) (ref. 12).

CONCLUSIONS

1. Coating substrate interdiffusion between the Ni-16Cr-25Al-0.06Zr coating and Ni-22Cr substrate rapidly reduced the Al content of the coating and resulted in considerable porosity at the coating/substrate interface following cyclic oxidation at 1150° C.

2. A numerical model (COSIM) was developed and shown to predict, with reasonable success, coating degradation by simultaneous oxidation and coating/substrate interdiffusion.

3. The ability of the COSIM numerical model to identify critical system parameters was demonstrated for the case of the initial Al and Cr contents of both the coating and substrate.

ACKNOWLEDGMENTS

The authors would like to acknowledge the discussions and help of M. A. Gedwill, S. R. Levine, and C. E. Lowell of the Lewis Research Center, Cleveland, OH, and also the help of M. R. Jackson of the General Electric Research and Development Center, Schenectady, NY, with the coating application.

REFERENCES

1. G. W. Goward, in Source Book on Materials for Elevated-Temperature Applications, compiled by Elihu F. Bradley (American Society for Metals, Metals Park, OH, 1979), pp. 369-386.

2. S. Shankar, D. e. Koenig and L. E. Dardi, J. Met. 33 (10), 13 (1981).

3. S. C. Singhal (ed.), High-Temperature Protective Coatings, (Metallurgical Society of AIME, Warrendale, PA, 1982).

4. P. G. Cappelli, in High Temperature Alloys for Gas Turbines, edited by D. Coutsouradis, P. Felix, H. Fischmeister, L. Habraken, Y. Lindblom, and M. O. Speidel (Applied Science Publishers, London, England, 1978), p. 177-189.

5. S. Stecura, Am. Ceram. Soc. Bull. 56, 1082 (1977).

6. C. A. Barrett, A. S. Khan, and C. E. Lowell, J. Electrochem, Soc. 128, 25 (1981).

7. I. M. Allam, D. P. Whittle, and J. Stringer, Oxid. Met, 13, 381 (1979).

8. S. R. Levine, Met. Trans. A 9, 1237 (1978).

9. F. S. Pettit, Trans. Metall. Soc. AIME 239, 1296 (1967).

10. C. S. Giggins and F. S. Pettit, J. Electrochem, Soc,. 118, 1782 (1971).

11. J. A. Nesbitt and R. W. Heckel, in High-Temperature Protective Coatings, edited by S. C. Singhal (Metallurgical Society of AIME, Warrendale, PA, 1982), p. 75-91.

12. J. A. Nesbitt, Ph.D dissertation, Michigan Technological University, Houghton, MI, 1983.

13. C. A. Barrett and C. E. Lowell, Oxid. Met. 11, 199 (1977).

14. A. J. Hickl and R. W. Heckel, Met. Trans. A 6, 431 (1975).

15. J. I. Goldstein and E. Randich, Met. Trans. A 8, 105 (1977).

16. C. E. Lowell, J. L. Smialek, and C. A. Barrett, in High Temperature Corrosion, edited by Robert A. Rapp (National Association of Corrosion Engineers, Houston, TX, 1983), p. 219-226.

TABLE I. - OXIDE PHASES PRESENT ON THE SPECIMEN SURFACE AFTER CYCLIC OXIDATION AT 1150° C

	Number of 1-hour cycles		
	100	200	250
Oxide (major)	Al_2O_3	Al_2O_3	Cr_2O_3
Phases (minor)	$NiAl_2O_4$	$NiAl_2O_4$ NiO $NiCr_2O_3$ Cr_2O_3	$NiAl_2O_4$

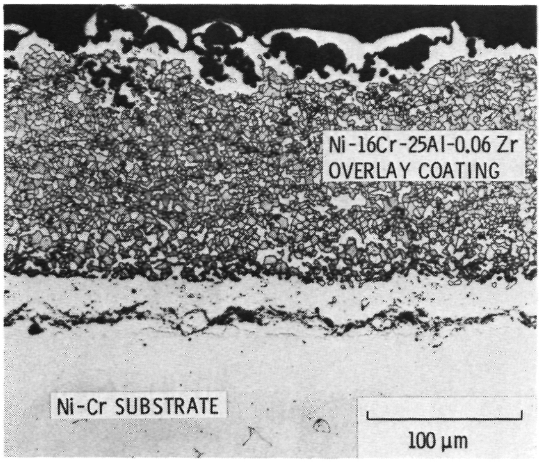

(a) Microstructure of the coating and substrate after a short anneal in Ar at 1150° C. (Cu and Ni plate are visible on the outer surface of the coating.)

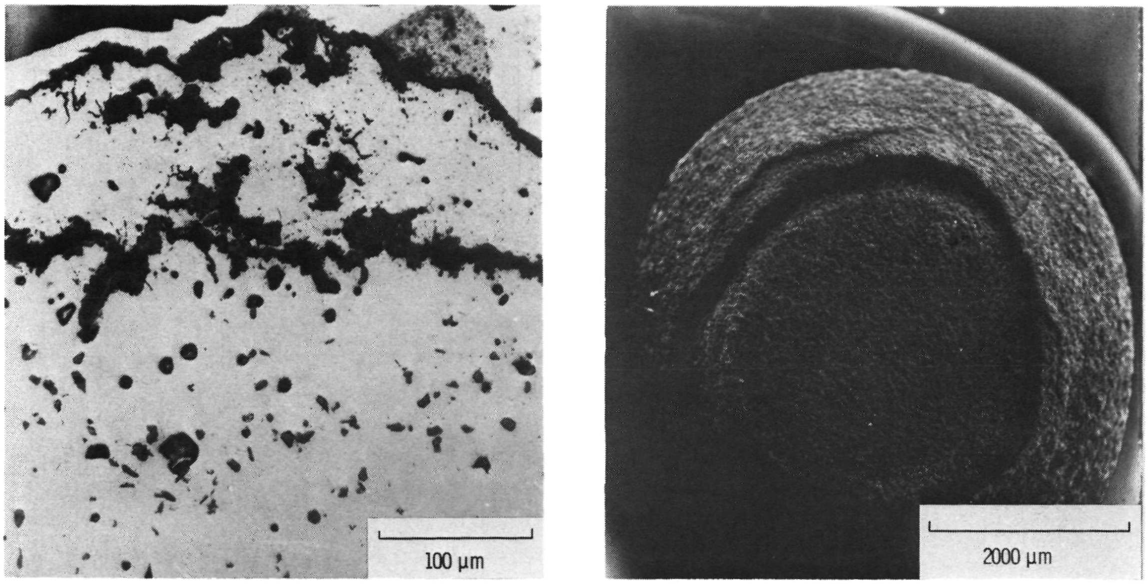

(b) Microstructure showing a cross section of the coating and Ni-22Cr substrate after 250 1-hour cycles at 1150° C. (Cu and Ni plate are visible on the outer surface of the coating.)

(c) SEM micrograph of the end of the cylindrical specimen showing coating spallation from the end of the cylinder after 250 1-hour cycles at 1150° C.

Figure 1. - Optical and scanning electron micrographs of a Ni-16Cr-25Al-0.06Zr overlay coating on a Ni-Cr substrate.

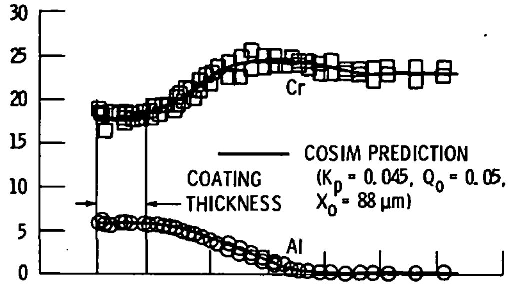

(a) After 100 1-hr cycles.

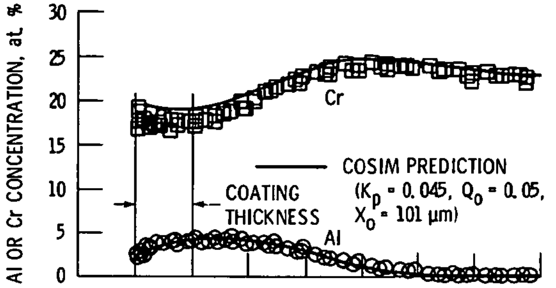

(b) After 200 1-hr cycles.

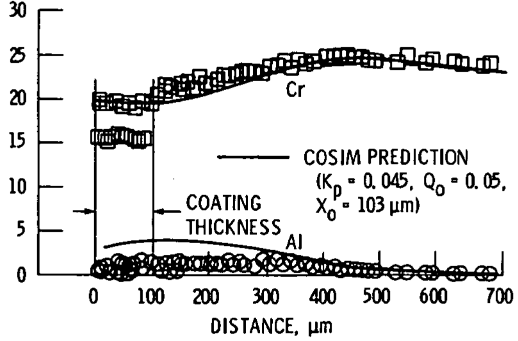

(c) After 250 1-hr cycles.

Figure 2. - Measured and predicted Al and Cr concentration/distance profiles. Test temperature, 1150° C; nominal compositions, at. %: Ni-22Cr substrate; Ni-16Cr-25Al coating. (K$_p$ = parabolic oxide growth constant; Q$_0$ = oxide spalling parameter (16); X$_0$ = coating thickness in micrometers.)

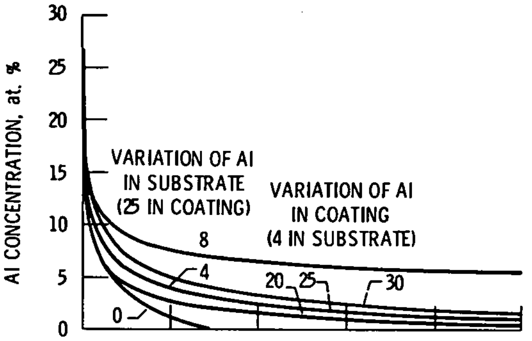

(a) Effect of Al concentration in substrate and coating. Nominal compositions, at. %: Ni-10 Cr -(0-8) Al substrate; Ni-15 Cr - (20-30) Al coating.

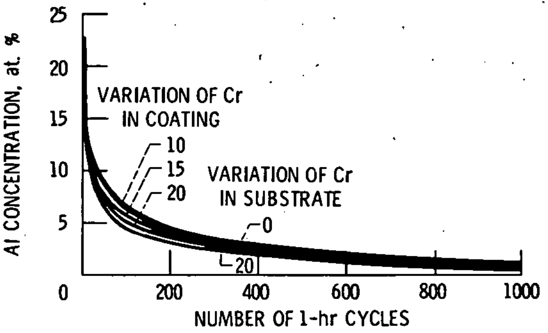

(b) Effect of Cr concentration in substrate and coating. Nominal compositions, at. %: Ni-(0-20) Cr - 4 Al substrate; Ni-(10-20) Cr - 25 Al coating.

Figure 3. - Effect of Al and Cr concentration on coating life. Al concentration plotted above is the concentration at the oxide/coating interface. Test temperature, 1150° C; coating thickness, 80 μm; COSP input: parabolic oxide growth constant, K$_p$ = 0.05; oxide spalling parameter, Q$_0$ = 0.005.

1. Report No. NASA TM-83672	2. Government Accession No.	3. Recipient's Catalog No.

4. Title and Subtitle Modeling Degradation and Failure of Ni-Cr-Al Overlay Coatings	5. Report Date
	6. Performing Organization Code 505-33-1A
7. Author(s) J. A. Nesbitt and R. W. Heckel	8. Performing Organization Report No. E-2116
	10. Work Unit No.
9. Performing Organization Name and Address National Aeronautics and Space Administration Lewis Research Center Cleveland, Ohio 44135	11. Contract or Grant No.
	13. Type of Report and Period Covered Technical Memorandum
12. Sponsoring Agency Name and Address National Aeronautics and Space Administration Washington, D.C. 20546	14. Sponsoring Agency Code

15. Supplementary Notes

J. A. Nesbitt, Lewis Research Center; R. W. Heckel, Michigan Technological University, Dept. of Metallurgical Engineering, Houghton, Michigan 49931 (work done under NASA grant NAS3-244). Prepared for the Eleventh International Conference on Metallurgical Coatings sponsored by the American Vacuum Society, San Diego, California, April 9-13, 1984.

16. Abstract

Degradation of a Ni-16Cr-25Al-0.06Zr overlay coating on a Ni-22Cr substrate was examined after oxidation accompanied by thermal cycling. Concentration/distance profiles were measured in the coating and substrate after various one-hour cycles at 1150° C. A numerical model was developed to simulate coating degradation by simultaneous oxidation and coating/substrate interdiffusion. The validity of the model was confirmed by comparison of predicted and measured concentration/distance profiles. The ability of the model to identify critical system parameters was demonstrated for the case of the initial Al and Cr content of the coating and substrate.

17. Key Words (Suggested by Author(s)) Overlay coatings Life prediction Cyclic oxidation Ni-Cr-Al alloys	18. Distribution Statement Unclassified - unlimited STAR Category 26

19. Security Classif. (of this report) Unclassified	20. Security Classif. (of this page) Unclassified	21. No. of pages	22. Price*

*For sale by the National Technical Information Service, Springfield, Virginia 22161

National Aeronautics and
Space Administration

Washington, D.C.
20546

Official Business
Penalty for Private Use, $300

SPECIAL FOURTH CLASS MAIL
BOOK

U.S. MAIL

Postage and Fees Paid
National Aeronautics and
Space Administration
NASA-451

NASA

POSTMASTER: If Undeliverable (Section 158
Postal Manual) Do Not Return